ISSN 1062-8738, Bulletin of the Russian Academy of Sciences: Physics, 2024, Vol. 88, Suppl. 3, pp. S340–S347. © Pleiades Publishing, Ltd., 2024.

Features of Degenerate Defect Modes in One-Dimensional Photonic Crystals with Two Defects

A. O. Kamenev[a, b, *] (ORCID: 0009-0006-8057-1170), N. A. Vanyushkin[b] (ORCID: 0000-0003-2338-680X), I. M. Efimov[b] (ORCID: 0000-0001-6793-704X), S. S. Golik[a, b] (ORCID: 0000-0003-4199-4163), and A. H. Gevorgyan[b, c] (ORCID: 0000-0002-0438-0069)

[a] *Institute of Automation and Control Processes, Far Eastern Branch, Russian Academy of Sciences, Vladivostok, 690041 Russia*

[b] *Institute of High Technologies and Advanced Materials, Far Eastern Federal University, Vladivostok, 690922 Russia*

[c] *Il'ichev Pacific Oceanological Institute, Far Eastern Branch, Russian Academy of Science, Vladivostok, 640041 Russia*

**e-mail: kamenev.ao@dvfu.ru*

Received October 31, 2024; revised November 15, 2024; accepted November 28, 2024

Abstract—The different cases of degenerate defect modes in one-dimensional photonic crystals with two defect layers are studied. Degenerate defect modes occur when two or more defect modes merge at a given wavelength in the photonic crystal reflection spectrum. Such defect modes have a variety of potential practical applications, including the increase of sensitivity in optical sensors. The appearance of each type of degenerate defect modes is determined by the structural features and parameters of the photonic crystal. For this reason, we have derived analytical equations containing the photonic crystal parameters describing each type of defect modes merging. Analytical expressions for the zero imaginary phase for any type of defect mode merging have been also obtained. These general relationships can be used to simplify the modeling of one-dimensional photonic crystals with two defect layers and for further analysis of degenerate defect modes.

Keywords: binary photonic crystals, photonic band gap, degenerate defect modes, coupled resonators

DOI: 10.1134/S1062873824709796

INTRODUCTION

The rapid development of optics and photonics in recent years has led to more and more new research into the use of different materials and advanced structures to control light and create various high-tech devices. As a result, a number of interesting properties of photonic crystals (PCs) have been discovered. These structures are artificially created or self-organizing nanostructures with periodic refractive index changes in one (1D PC), two (2D PC) or three (3D PC) spatial dimensions [1, 2]. A well-known property of such structures is their ability to control the light passing through them, among other things, due to the presence of so-called photonic bandgap (PBG), which are wavelength ranges where light propagation through PCs is impossible [3–5]. Many optical devices have been developed that work thanks to the presence of PBGs in PCs: these are multichannel optical switches [6], filters [7], optical differentiators [8] and others. Violation of periodicity of 1D PCs by adding one or more defect layers (DLs) allows to further extend the range of applications of such structures. This is made possible by the appearance of a narrow defect mode (DM) within their PBG, which in 1D PCs represents a resonant peak in the transmission spectra. The number of DMs within the PBG is determined by the number of DLs in the structure of the PC and their optical thicknesses. The parameters of the DLs directly influence the position of the DMs in the PC spectra, which is the basis for the operation of 1D PC-based sensors. Over the past few decades, many different optical sensors based on 1D PCs with DLs have been developed for a wide range of applications. These include gas sensors [9], sensors for refractive index of liquids [10], temperature sensors [11], biochemical sensors [12] and sensors for the detection of harmful viruses and bacteria in the human body [13]. Additionally, many papers have been published on the optimization of 1D PCs and their properties [14–18].

Nevertheless, most researchers deal with PC structures containing only one DL. However, adding more DLs allows to expand the application possibilities of such PCs. One of the obvious applications of such structures is their promising potential as optical filters due to the possibility of independent manipulation of two or more DMs by varying the number and thickness of DLs in the PC structure [19] or tuning their

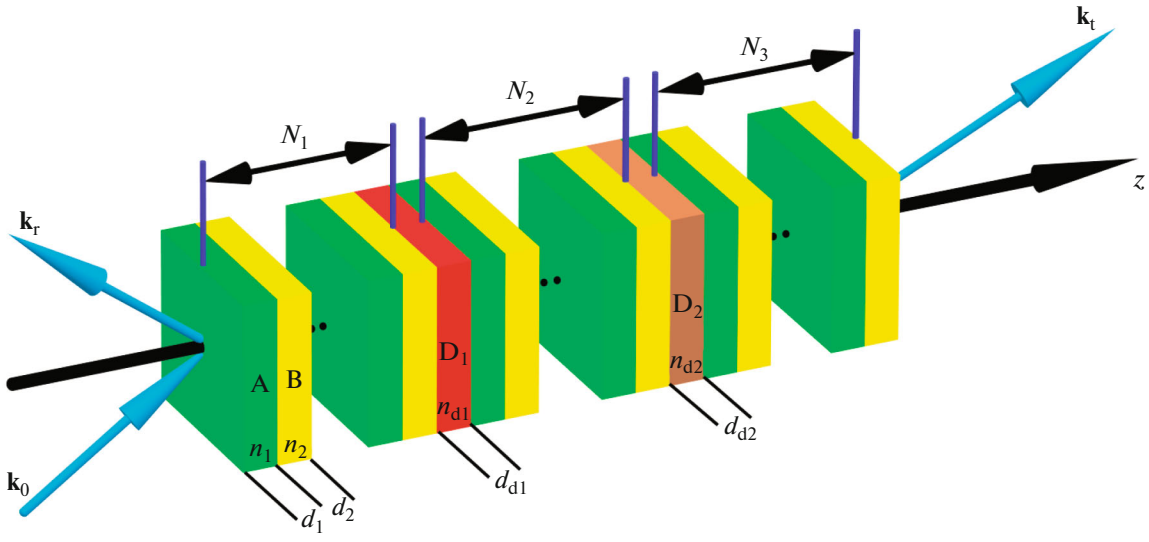

Fig. 1. Geometry of the problem using the example of a structure without MS (mirror symmetry) (AB|D_1|AB|D_2|AB). Here $\mathbf{k_0}$, $\mathbf{k_r}$, $\mathbf{k_t}$ are the wave vectors of the incident, reflected and transmitted waves, respectively.

properties by an external (electric, magnetic, light, mechanical, temperature, etc.) field, or by changing their position in the PC layer. In addition, in [20, 21], the advantages of 1D PCs with two DLs to create ultrafast all-optical switching devices and broadband energy localization under the action of elastic waves have been shown. And in [22, 23], researchers have demonstrated the promising potential of 1D PCs with two DLs for creating temperature sensors and sensors for biomedical applications.

There is a particular interest in the phenomenon of DM merging in 1D PCs with two DLs. Such a structure can be considered as a coupled resonator system with an exceptional point of degeneracy (EPD) [24]. At this point, for certain parameters of the structure, a degenerate DM can arise. Other researchers have shown that such a mode can have a number of interesting properties, including increased sensitivity to changes in system parameters and the achievement of the gain enhancement in a Fabry–Pérot cavity [25–27]. Among others, in [28] the authors have reviewed the opportunities offered by exceptional point physics in photonics, discussed recent developments in theoretical and experimental research based on photonic exceptional points, and examined future opportunities in this field from basic science to applied technology. However, the EPDs in 1D PCs with two DLs are not well studied. For this reason, the present work is dedicated to investigating the details of the mode merging. This work is the second part of our broad study and complements the conclusions we obtained in [29]. In the present study, analytical equations describing each type of merging modes are derived for the first time, and analytical conditions for the merging of DMs in a 1D PC with two DLs are expanded and supplemented. The obtained expressions can be used in the future for a simplifying of modeling of such structures with EPD, as well as for an unambiguous search for the PC parameters at which this phenomenon is observed.

THE MODEL OF 1D PC WITH TWO DEFECT LAYERS

Figure 1 shows a defected 1D binary PC which consists of two DLs with refractive indices n_{d1} and n_{d2}. The thicknesses of the DLs (d_{d1} and d_{d2}) are stacked sequentially between three PCs, which are made of N_1, N_2 and N_3 unit cells each and playing the role of mirrors. The unit cell consists of layer A with refractive index n_1 and thickness d_1 and layer B with refractive index n_2 and thicknessd_2. For clarity we will assume that $n_2 > n_1$ throughout the paper. The regions outside the structure are filled with air ($n_0 = 1$). Depending on the order of alternation of layers and the arrangement of DLs inside the PC, the structure will have one or another type of symmetry and different properties.

For numerical modeling of electromagnetic radiation propagation through a 1D PC with two DLs, we used the well-known transfer-matrix method [30]. This method is based on the fact that for each PC layer a transfer matrix M_j, depending on the PC parameters, is written:

$$M_j = \begin{pmatrix} \cos k_j d_j & \frac{-i}{p_j}\sin k_j d_j \\ -ip_j \sin k_j d_j & \cos k_j d_j \end{pmatrix}, \quad (1)$$

where $k_j = \frac{\omega}{c} n_j \cos\theta_j$, d_j is the thickness of the jth layer, θ_j is the angle of refraction which is determined from Snell's law as: $n_j \sin\theta_j = n_0 \sin\theta_0$, n_0 is the refractive index of the external medium from where the wave is incident, θ_0 is angle of incidence, $p_j = n_j \cos\theta_j$. Then the transfer matrix m of a PC consisting of N layers can be obtained by multiplying the transfer matrices of all layers:

$$m = \prod_{j=1}^{N} M_j = \begin{pmatrix} m_{11} & m_{12} \\ m_{21} & m_{22} \end{pmatrix}. \quad (2)$$

The complex reflection amplitudes are given as:

$$r = \frac{(m_{11} + m_{12} p_0) p_0 - (m_{21} + m_{22} p_0)}{(m_{11} + m_{12} p_0) p_0 + (m_{21} + m_{22} p_0)}, \quad (3)$$

where $p_0 = n_0 \cos\theta_0$. And the corresponding reflection coefficients are defined as: $R = |r|^2$.

The DL transfer matrix without considering the reflection from the boundaries will then take the following form:

$$M_d = \begin{pmatrix} e^{-i\varphi} & 0 \\ 0 & e^{i\varphi} \end{pmatrix}, \quad (4)$$

where

$$\varphi = \frac{2\pi}{\lambda} n_d d_d. \quad (5)$$

φ is the change of phase of the wave at a single passage through the DL. It should be noted that the phase change will vary for each DL. Consequently, for two DLs in the PC structure, we can express this as follows: $\varphi_1 = \frac{2\pi}{\lambda} n_{d1} d_{d1}$, $\varphi_2 = \frac{2\pi}{\lambda} n_{d2} d_{d2}$. It follows that the actual total phase is equal to $\varphi'_m = \varphi_1 + \varphi_2 = \frac{2\pi}{\lambda}(n_{d1} d_{d1} + n_{d2} d_{d2})$.

Below, we use the following notations: the coefficients r, t are the reflection and transmission coefficients, index I denotes the perfect PC to the left of the first DL, index II denotes the perfect PC between the first and second DLs, and index III denotes the perfect PC to the right of the second DL. Thus, the transfer matrix of a PC with two DLs can be generally represented as:

$$m = M_I M_{d1} M_{II} M_{d2} M_{III}, \quad (6)$$

where M_I, M_{II} and M_{III} are the transfer matrices of left, central and right mirror' and M_{d1}, M_{d2} are "inner" transfer matrices of first and second DLs.

TYPES OF DEGENERATE DEFECT MODES AND DERIVATION OF THE CONDITION FOR THE MERGE

In our previous work [29], we have obtained analytical expressions for determination of the wavelength of DMs in 1D PCs with two DLs, and found two solutions to the equation for the required total phase, each of which can be compared to the behavior of each of the two DMs arising in such structures. These solutions are given by equation:

$$\varphi_{m_{1,2}} = -i \ln\left[\frac{1}{2}\left(\frac{\tilde{r}_{II}^*}{r_{III}} e^{i\Delta\varphi} + \frac{\tilde{r}_I^*}{r_{II}} e^{-i\Delta\varphi} |r_{II}|^2 \pm \sqrt{\left(\frac{\tilde{r}_{II}^*}{r_{III}} e^{i\Delta\varphi} + \frac{\tilde{r}_I^*}{r_{II}} e^{-i\Delta\varphi} |r_{II}|^2\right)^2 - \frac{4\tilde{r}_I^* \tilde{r}_{II}^*}{r_{II} r_{III}}}\right)\right] + 2\pi q_1, \quad (7)$$

where $q_1 \in \mathbb{Z}$.

Here $\tilde{r}_I^* = -r_I t_I^* / t_I$, $\tilde{r}_{II}^* = -r_{II} t_{II}^* / t_{II}$, $\Delta\varphi = \varphi_1 - \varphi_2$. These solutions for the DL phase are periodical in $\Delta\varphi$ with the period 2π, and the integer number q_1 can be associated with the DM order [17]. So, φ_m shows what φ'_m should be equal to achieve zero reflection coefficients at a given wavelength and mirrors' parameters.

Figure 2a shows the reflectance spectrum $|R|^2$ of 1D PC with two DLs (black) obtained using the transfer matrix method for the structure $(AB|D_1|BA|D_2|AB)$ and also spectra of Re$[\varphi_m - \varphi'_m]$ (red) and Im $[\varphi_m]$ (blue). In this structure and at these PC parameters the merging of DMs is not observed.

Fig. 2. Spectra of Re$[\varphi_m - \varphi'_m]$ (red), Im$[\varphi_m]$ (blue), and reflection spectrum $|R|^2$ (black) for the structures (a) $(AB|D_1|BA|D_2|AB)$, (c) $(AB|D_1|AB|D_2|BA)$, (e) $(BA|D_1|AB|D_2|BA)$. Reflection spectrum $|R|^2$ (black), spectra of function ξ (green), function Arg c (blue) and function $|c|$ (red) for the structures (b) $(AB|D_1|BA|D_2|AB)$, (d) $(AB|D_1|AB|D_2|BA)$, (f) $(BA|D_1|AB|D_2|BA)$. The parameters of the structures are (a, b) $N_1 = N_2 = N_3 = 5$, $n_1 = 1.5$, $n_2 = 2.4$, $d_1 = 123$ nm, $d_2 = 77$ nm, $d_{d1} = d_{d2} = 0$, $n_{d1} = n_{d2} = 1.33$; (c, d) $N_1 = N_3 = 9$, $N_2 = 14$, $n_1 = 1.8$, $n_2 = 2.0$, $d_1 = 210.5$ nm, $d_2 = 189.5$ nm, $d_{d1} = 248.6$ nm, $d_{d2} = 0$, $n_{d1} = n_{d2} = 1.52$; (e, f) $N_1 = 2$, $N_2 = 6$, $N_3 = 4$, $n_1 = 1.5$, $n_2 = 2.4$, $d_1 = 123$ nm, $d_2 = 77$ nm, $d_{d1} = 0$, $d_{d2} = 277.6$ nm, $n_{d1} = n_{d2} = 1.33$. The normal incidence of light on the PC was considered. The dashed lines mark the PBG center (this is the DM merging wavelength) and the boundaries of broadband merging.

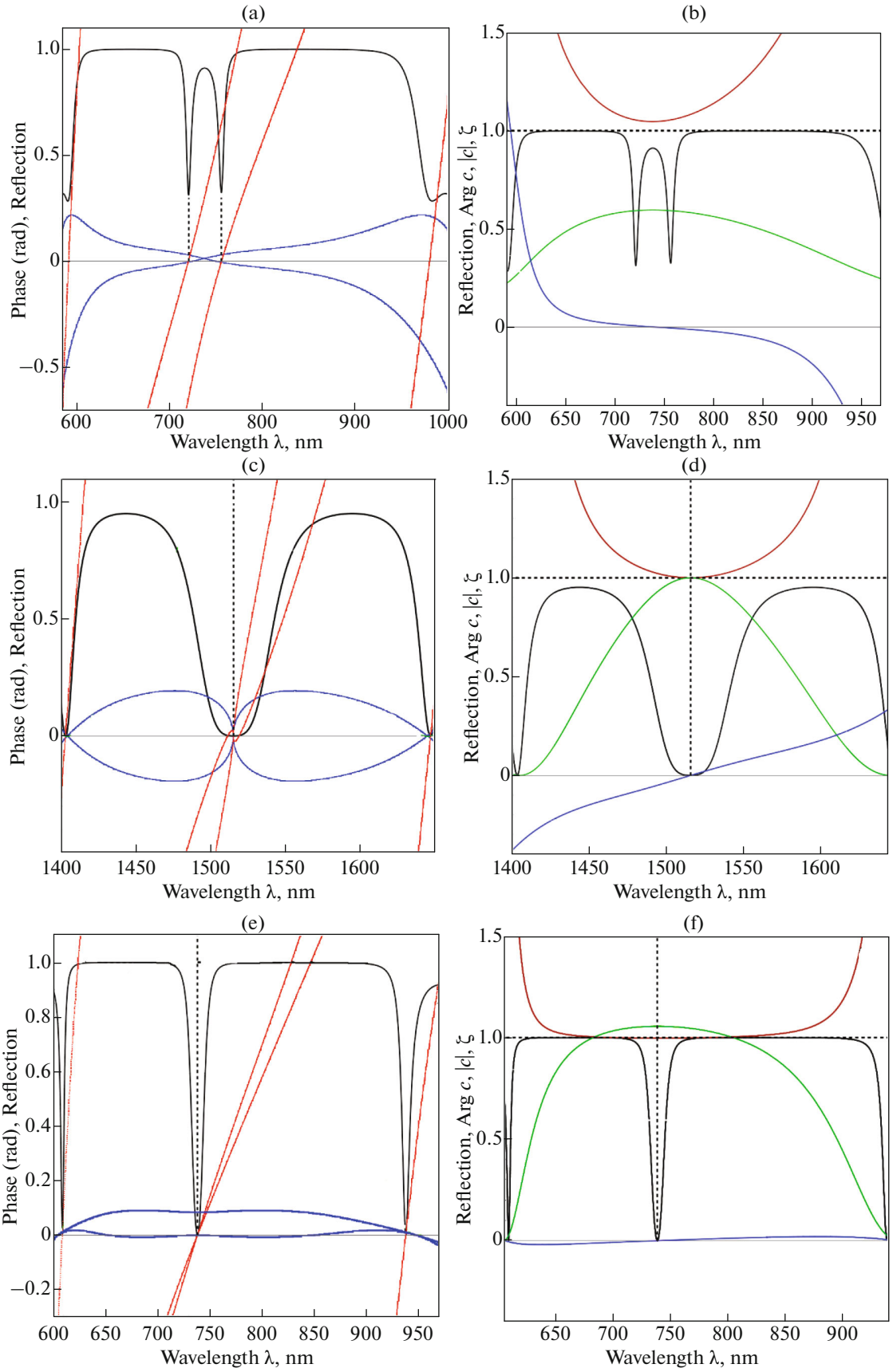
(a)
Phase (rad), Reflection
Wavelength λ, nm
(b)
Reflection, Arg c, |c|, ζ
Wavelength λ, nm
(c)
Phase (rad), Reflection
Wavelength λ, nm
(d)
Reflection, Arg c, |c|, ζ
Wavelength λ, nm
(e)
Phase (rad), Reflection
Wavelength λ, nm
(f)
Reflection, Arg c, |c|, ζ
Wavelength λ, nm

Let us simplify the Eq. (7):

$$b = \frac{\tilde{r}_{II}^*}{r_{III}} e^{i\Delta\varphi} + \frac{\tilde{r}_I^*}{r_{II}} e^{-i\Delta\varphi} |r_{II}|^2, \; a = \frac{\tilde{r}_I^* \tilde{r}_{II}^*}{r_{II} r_{III}}, \; D = b^2 - 4a. \quad (8)$$

This substitution leads to the following equation:

$$\varphi_{m_{1,2}} = -i \ln\left[\frac{1}{2}\left(b \pm \sqrt{D}\right)\right] = \mathrm{Arg}\left(\frac{1}{2}\left(b \pm \sqrt{D}\right)\right) - i \ln\left|\frac{1}{2}\left(b \pm \sqrt{D}\right)\right| + 2\pi q_1. \quad (9)$$

For DM merging, equality of the real parts of the solution (9) is necessary. And for this it is necessary to fulfil equality:

$$\mathrm{Arg}\left(\frac{1}{2}\left(b + \sqrt{D}\right)\right) = \mathrm{Arg}\left(\frac{1}{2}\left(b - \sqrt{D}\right)\right) + 2\pi q, \quad (10)$$

where $q \in \mathbb{Z}$.

Therefore

$$\mathrm{Arg}\left(\frac{b + \sqrt{D}}{b - \sqrt{D}}\right) = \mathrm{Arg}\frac{a}{\left(b - \sqrt{D}\right)^2} = \mathrm{Arg}\frac{c}{1 - \sqrt{1 - c^2}} = 2\pi q, \quad (11)$$

where $c = 2\sqrt{a}/b$. The general solution of equation (11) with respect to c can be found, for example, graphically, and it is the following system:

$$\begin{cases} \mathrm{Arg} c = 2\pi q, \\ 0 \le |c| \le 1. \end{cases} \quad (12)$$

The function c depends on $\Delta\varphi$ and reflection coefficients of each mirror in the 1D PC structure with two DLs, and thus, using the system (12) it is possible to select such PC parameters at which one or another type of DM merging will be observed at a given wavelength or in a particular wavelength range.

The system (12) in the limiting case corresponds to the equation $c = 1$. It follows from (8) that $D = 0$. The equation has been solved in [29]. There we have obtained a condition on the touching of the phase curves at which DMs merge:

$$\Delta\varphi = \frac{1}{2}(\tilde{\rho}_{II} - \rho_{II} + \rho_{III} - \tilde{\rho}_I) - \frac{1}{2} i \ln\left[\frac{2 - |r_{II}|^2 \pm 2\sqrt{1 - |r_{II}|^2}}{|r_{II}|^2 |r_{III}||r_I|}\right] + \pi q_2, \quad (13)$$

where $q_2 \in \mathbb{Z}$, $\rho = \mathrm{Arg}(r)$ is the phase of reflection coefficients: $r = |r| e^{i\rho}$. In this solution, we can identify an important function ξ, whose wavelength dependence can characterize one or another type of DM merging:

$$\xi = \frac{2 - |r_{II}|^2 - 2\sqrt{1 - |r_{II}|^2}}{|r_{II}|^2 |r_{III}||r_I|}. \quad (14)$$

Thus, these two equations ($c = 1$ and $D = 0$) are essentially equivalent and describe from different sides the phenomenon of EPD in 1D PC with two DLs. The real part of the solution of $\Delta\varphi$ is responsible for Arg$c$ and the imaginary part for $|c|$. It can be shown that if $\xi \ge 1$ at a given wavelength, then there is such a value of $\Delta\varphi$ at which $|c| \le 1$ at the same wavelength and DM merging occurs.

Now, to expand the understanding of the DMs merging we have analyzed various cases of DM merging in 1D PC with two DLs and identified the following main types: (1) DM touching; (2) DM intersection; (3) perfect broadband merging; (4) incomplete broadband merging. Figures 2 and 3 show examples of different types of DM merging on the reflectance spectrum: touching (2b), intersection (2c), incomplete broadband merging (3a) and perfect broadband merging (3b). The difference between incomplete and perfect merging is that the total phase solutions only coincide at one wavelength and diverge slightly in the vicinity.

Also, Figs. 2 and 3 show the correspondence between each type of DM merging (the corresponding reflection spectrum (black) $|R|^2$), as well as the absence of merging, and the wavelength dependence of the function ξ (green), the function Arg c (blue), and the function $|c|$ (red). It can be said that for DM merging at one wavelength or in a range of wavelengths it is necessary that the condition $\xi \ge 1$ is fulfilled. It is well seen that when there is no mode merging (Figs. 2a, 2b), ξ is always less than unity, $|c|$ is always more than unity and Arg$c = 0$ only in the center of the PBG. For DM touching (Figs. 2c, 2d), ξ and $|c|$ are equal to unity only in the center of the PBG, and Arg$c = 0$ only in the center of the PBG. For DM intersection (Figs. 2e, 2f), ξ is more than unity in the region of the PBG center, $|c| = 1$ and Arg$c = 0$ only in the center of the PBG. For incomplete broadband merging (Figs. 3a, 3b), ξ is more than unity, $|c|$ is less than unity in the region of the incomplete merging, and Arg$c = 0$ only in the PBG center. Finally, for perfect broadband merging (Figs. 3c, 3d), ξ is more than unity, $|c|$ is less than unity in the region of the broadband merging, and Arg$c = 0$ over the whole wavelength range. Thus, the behavior of these functions determines each type of DM merging.

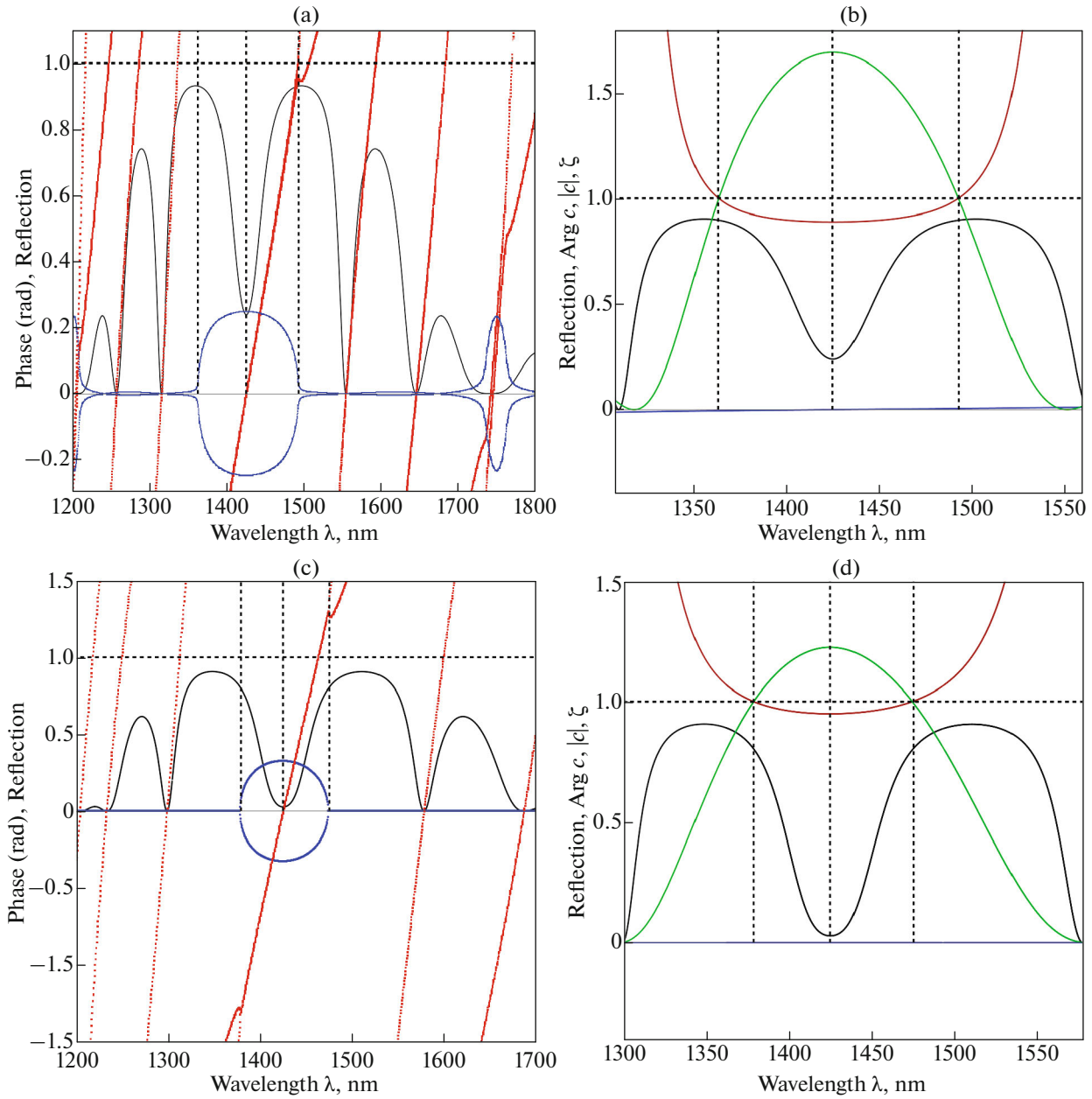

Fig. 3. Spectra of $\mathrm{Re}[\varphi_m - \varphi_m']$ (red), $\mathrm{Im}[\varphi_m]$ (blue), and reflection spectrum $|R|^2$ (black) for the structures (a) AB|D_1|AB|D_2|BA and (c) AB|D_1B|AB|D_2|BA. Reflection spectrum $|R|^2$ (black), spectra of function ξ (green), function Arg c (blue) and function $|c|$ (red) for the structures (b) AB|D_1|AB|D_2|BA and (d) AB|D_1B|AB|D_2|BA. The parameters of the structures are (a, b) $N_1 = N_3 = 6$, $N_2 = 14$, $n_1 = 1.34$, $n_2 = 1.52$, $d_1 = 265.5$ nm, $d_2 = 234.5$ nm, $d_{d1} = 267.8$nm, $d_{d2} = 535.6$ nm, $n_{d1} = n_{d2} = 1.3$; (c, d) $N_1 = N_3 = 6$, $N_2 = 10$, $n_1 = 1.34$, $n_2 = 1.52$, $d_1 = 265.5$ nm, $d_2 = 234.5$ nm, $d_{d1} = 536$ nm, $d_{d2} = 536$ nm. The normal incidence of light on the PC was considered. The dashed lines mark the PBG center (this is the DM merging wavelength) and the boundaries of broadband merging.

ANALYTICAL EQUATIONS FOR THE ZERO IMAGINARY PHASE FOR DM MERGING

In our previous paper [29], we have already shown the influence of the imaginary part of the total phase $\mathrm{Im}[\varphi_m]$ from Eq. (7) on the DM amplitude in the reflection spectrum of a 1D PC with two DLs. A high value of the imaginary part of the total phase decreases the DM amplitude. To achieve the maximum amplitude of the DM, a zero value of the imaginary phase is

necessary in structures with real values of the refractive indices of the PC layers. We have obtained the following condition on the zero imaginary phase:

$$\frac{|b|^2+|D|-4}{2|b|\sqrt{|D|}}=\pm\cos\left(\mathrm{Arg}[b]-\frac{1}{2}\mathrm{Arg}[D]\right). \quad (15)$$

Now, we can simplify this condition for any type of DM merging. Taking into account Eq. (8)

$$\begin{aligned}&\cos\left(\mathrm{Arg}[b]-\frac{1}{2}\mathrm{Arg}[D]\right)\\ &=\cos\left(\mathrm{Arg}[b]-\frac{1}{2}\mathrm{Arg}\left[b^2\left(1-c^2\right)\right]\right)\\ &=\cos\left(\mathrm{Arg}[b]-\frac{1}{2}\mathrm{Arg}\left[b^2\right]\right)=1,\end{aligned} \quad (16)$$

$$\frac{|b|^2+|D|-4}{2|b|\sqrt{|D|}}=\frac{|b|^2+|b|^2\left(1-c^2\right)-4}{2|b|^2\sqrt{1-c^2}}. \quad (17)$$

Therefore:

$$|b|=\frac{2}{1\pm\sqrt{1-c^2}} \quad (18)$$

or equivalently

$$|a|=\frac{c^2}{\left(1\pm\sqrt{1-c^2}\right)^2}. \quad (19)$$

Using Eqs. (18) and (19), it is possible to select such parameters of the PC structure at which the imaginary total phase equals zero at the necessary wavelength for any type of DM merging.

CONCLUSIONS

We have investigated and analyzed different types of degenerate DMs arising in a system of two coupled resonators comprised of a 1D PC with two DLs. A total of four main types of DM merging have been found: (1) DM touching; (2) DM intersection; (3) perfect broadband merging; (4) incomplete broadband merging. We have obtained the analytical condition for the occurrence of each type of degenerate DMs. Also, analytical conditions on the merging DMs with zero value of the reflection coefficient were obtained. Using these conditions, it is possible to find such parameters of the PC at which the merging of DMs is observed in the reflection spectrum. This greatly simplifies the study of 1D PCs with two DLs and opens new perspectives for the modeling and analysis of degenerate DMs in such structures, as well as the search for new effects.

FUNDING

For AHG the work was carried out within the framework of the state projects: reg. no. 1240423000003-5.

CONFLICT OF INTEREST

The authors of this work declare that they have no conflicts of interest.

REFERENCES

1. Krauss, T.F. and Richard, M., *Prog. Quantum Electron.*, 1999, vol. 23, no. 2, p. 51. https://doi.org/10.1016/S0079-6727(99)00004-X
2. Yablonovitch, E., *J. Mod. Opt.*, 1994, vol. 41, no. 1, p. 173. https://doi.org/10.1080/09500349414550261
3. Xiao, M., Zhang, Z., and Chan, C., *Phys. Rev. X*, 2014, vol. 4, no. 2, p. 021017. https://doi.org/10.1103/PhysRevX.4.021017
4. Fenzl, C., Hirsch, T., and Wolfbeis, O.S., *Angew. Chem., Int. Ed.*, 2014, vol. 53, no. 12, p. 3318. https://doi.org/10.1002/anie.201307828
5. Vanyushkin, N.A. and Gevorgyan, A.H., *Bull. Russ. Acad. Sci.: Phys.*, 2022, vol. 86, no. 1, p. 243. https://doi.org/10.3103/S1062873822700769
6. Wu, C.Y., Zou, Y.H., Timofeev, I.V., Lin, Y.T., Zyryanov, V.Y., Hsu, J.S., and Lee, W., *Opt. Express*, 2011, vol. 19, no. 8, p. 7349. https://doi.org/10.1364/OE.19.007349
7. Jena, S., et al., *Phys. E*, 2019, vol. 114, no. 1, p. 113627. https://doi.org/10.1016/j.physe.2019.113627
8. Kashapov, A.I., Bezus, E.A., Bykov, D.A., et al., *Bull. Russ. Acad. Sci.: Phys.*, 2023, vol. 87, no. 1, p. 13. https://doi.org/10.3103/S1062873822700034
9. Zhang, Y., Zhao, Y., and Wang, Q., *Sens. Actuators, B*, 2013, vol. 184, no. 1, p. 179. https://doi.org/10.1016/j.snb.2013.04.082
10. Lai, W.C., Chakravarty, S., Zou, Y., et al., *Opt. Lett.*, 2013, vol. 38, no. 18, p. 3799. https://doi.org/10.1364/OL.38.003799
11. Soltani, A., Ouerghi, F., AbdelMalek, F., and Haxha, S., *Opt. Commun.*, 2019, vol. 445, no. 1, p. 268. https://doi.org/10.1016/j.optcom.2019.04.056
12. Zheng, S., Zhu, Y., and Krishnaswamy, S., *Proc. SPIE*, 2012, vol. 8346, no. 1, p. 83460D. https://doi.org/10.1117/12.915050
13. Efimov, I.M., et al., *Phys. Scr.*, 2022, vol. 97, no. 5, p. 055506. https://doi.org/10.1088/1402-4896/ac5ff7
14. Efimov, I.M., et al., *Comput. Opt.*, 2023, vol. 47, no. 4, p. 572. https://doi.org/10.18287/2412-6179-CO-1245
15. Efimov, I.M., Vanyushkin, N.A., and Gevorgyan, A.H., *Photonics*, 2024, vol. 11, no. 1, p. 56. https://doi.org/10.3390/photonics11010056
16. Vanyushkin, N.A., Gevorgyan, A.H., and Golik, S.S., *Optik*, 2021, vol. 242, no. 1, p. 167343. https://doi.org/10.1016/j.ijleo.2021.167343
17. Kamenev, A.O., et al., *Phys. Scr.*, 2024, vol. 99, no. 4, p. 045521. https://doi.org/10.1088/1402-4896/ad32fc
18. Efimov, I.M., Vanyushkin, N.A., and Gevorgyan, A.H., *Bull. Russ. Acad. Sci.: Phys.*, 2022, vol. 86, suppl. 1, p. S60. https://doi.org/10.3103/S1062873822700393

19. Hsu, H.T., et al., *Prog. Electromagn. Res.*, 2011, vol. 117, no. 1, p. 379. https://doi.org/10.2528/PIER11051403
20. Ma, G., et al., *Opt. Express*, 2006, vol. 14, no. 2, p. 858. https://doi.org/10.1364/OPEX.14.000858
21. Jo, S.H., et al., *Int. J. Mech. Sci.*, 2020, vol. 183, no. 1, p. 105833. https://doi.org/10.1016/j.ijmecsci.2020.105833
22. El-Ghany, S.E.S.A., *J. Nanoelectron. Optoelectron.*, 2018, vol. 13, no. 2, p. 221. https://doi.org/10.1166/jno.2017.2199
23. Bissa, S., et al., *Mater. Today: Proc.*, 2022, vol. 62, no. 1, p. 5407. https://doi.org/10.1016/j.matpr.2022.03.616
24. Nikzamir, A. and Capolino, F., *Phys. Rev. Appl.*, 2022, vol. 18, no. 5, p. 054059. https://doi.org/10.1103/PhysRevApplied.18.054059
25. Kazemi, H., Hajiaghajani, A., Nada, M.Y., Dautta, M., Alshetaiwi, M., Tseng, P., and Capolino, F., *IEEE Sens. J.*, 2021, vol. 21, no. 6, p. 7250. https://doi.org/10.1109/JSEN.2020.3047886
26. Nada, M.Y., Othman, M.A.K., and Capolino, F., *Phys. Rev. B*, 2017, vol. 96, no. 18, p. 184304. https://doi.org/10.1103/PhysRevB.96.184304
27. Othman, M.A.K., Yazdi, F., Figotin, A., and Capolino, F., *Phys. Rev. B*, 2016, vol. 93, no. 2, p. 024301. https://doi.org/10.1103/PhysRevB.93.024301
28. Miri, M.A. and Alu, A., *Science*, 2019, vol. 363, no. 6422, p. eaar7709. https://doi.org/10.1126/science.aar7709
29. Kamenev, A.O., et al., *arXiv preprint*, 2024, vol. 2408, p. 04397. https://arxiv.org/abs/2408.04397.
30. Yeh, P., *Optical Waves in Layered Media*, New York: Wiley, 1988.

Publisher's Note. Pleiades Publishing remains neutral with regard to jurisdictional claims in published maps and institutional affiliations.
AI tools may have been used in the translation or editing of this article.